1   **Flow cytometric analysis and purification of airway epithelial cell subsets**

2

3   Luke R. Bonser[1,2], Kyung Duk Koh[1,2], Kristina Johansson[3,4,5], Semil P. Choksi[2], Dan Cheng[1,2,9],

4   Leqian Liu[6], Dingyuan I. Sun[7], Lorna T. Zlock[7], Walter L. Eckalbar[1,8], Walter E. Finkbeiner[7], and

5   David J. Erle[1,2,8]

6

7   [1]Lung Biology Center, [2]Cardiovascular Research Institute, [3]Department of Microbiology and

8   Immunology, [4]Division of Pulmonary, Critical Care, Sleep, and Allergy, [5]Sandler Asthma Basic

9   Research Center, [6]Department of Bioengineering and Therapeutic Sciences, [7]Department of

10   Pathology, and [8]UCSF CoLabs, University of California San Francisco, San Francisco, CA

11   94143 and [9]Department of Respiratory and Critical Care Medicine, Renmin Hospital of Wuhan

12   University, Wuhan, China 430060

13

14   **Running title:** Flow cytometric analysis of the airway epithelium

15

16   Some of the results of these studies have been previously reported in the form of abstracts.

17

18   **Contributions:**

19   LRB and DJE contributed to study conception and design.

20   LRB developed novel experimental methods.

21   LRB, KJ, KDK, SPC, DC, LL, DIS, and LTZ performed experiments.

22   LRB, KJ, KDK, DC, LL, WLE, and DJE analyzed data.

23   LRB and DJE interpreted data.

24   WEF and DJE supervised study execution.

25   LRB, KDK, and DJE drafted the manuscript.

26   All authors revised the manuscript.

27 **Funding**

32 **Abstract**

33 The human airway epithelium is essential in homeostasis, and epithelial dysfunction contributes

34 to chronic airway disease. Development of flow cytometric methods to characterize subsets of

35 airway epithelial cells will enable further dissection of airway epithelial biology. Leveraging

36 single cell RNA-sequencing (scRNA-seq) data in combination with known cell type-specific

37 markers, we developed panels of antibodies to characterize and isolate the major airway

38 epithelial subsets (basal, ciliated, and secretory cells) from human bronchial epithelial cell

39 cultures. We also identified molecularly distinct subpopulations of secretory cells and

40 demonstrated cell subset-specific expression of low abundance transcripts and micro-RNAs that

41 are challenging to analyze with current scRNA-seq methods. These new tools will be valuable

42 for analyzing and separating airway epithelial subsets and interrogating airway epithelial

43 biology.

44

45 **Keywords**

46 Airway epithelium; single cell RNA sequencing; flow cytometry

Introduction

Flow cytometry is a commonly used research and diagnostic tool that uses fluorophore-conjugated antibodies as probes to identify, characterize, and/or isolate cell populations (1). The immunology community has developed panels of antibodies useful for detailed immunophenotyping of immune cells derived from many organs including the lung. A recent American Thoracic Society working group report (2) heralded the importance of flow cytometry in pulmonary research, but noted that "the development of appropriate markers for nonimmunologic cells is less mature than other pulmonary cell types," including epithelial cells.

The airway epithelium defends against inhaled environmental challenges including pollutants, pathogens, and allergens (3), and epithelial dysfunction is central to the pathogenesis of major lung diseases including asthma, cystic fibrosis, chronic obstructive pulmonary disease, and primary ciliary dyskinesia (4). Proximal airway epithelial subsets including basal cells, ciliated cells, secretory cells including club and goblet cells, intermediate cells, brush cells, and pulmonary neuroendocrine cells have been defined morphologically and by their anatomical location within the tissue by histology and electron microscopy (5, 6). Single cell RNA-sequencing (scRNA-seq) is further advancing our understanding of airway epithelial heterogeneity. Recent studies of human and murine airways have confirmed the presence of previously defined major airway epithelial subsets, identified molecularly distinct subpopulations of these cells, and uncovered previously unrecognized cell types including ionocytes (7–11).

Pan-epithelial antibodies (EpCAM/pan-cytokeratin (12)) and limited sets of cell type-specific antibodies (e.g., acetylated alpha-tubulin (TUBA) for ciliated cells (13), nerve growth factor receptor (NGFR) and integrin subunit alpha 6 (ITGA6) (14) for basal cells, and mucin-5AC (MUC5AC) for goblet cells (15)) have been used individually for flow cytometry. We sought to develop a larger panel of antibodies for simultaneous analysis of the major subsets of airway epithelial cells and provide a new tool for further understanding airway epithelial physiology and

72   pathology. To this end, we used known markers described elsewhere in the literature,

73   augmented these by leveraging information from scRNA-seq datasets, and developed panels of

74   antibodies for flow cytometry to identify, characterize, and isolate the major human airway

75   epithelial subsets.

76

77   **Methods**

78   Additional details are provided in the online data supplement. A detailed protocol is provided in

79   the online supplementary document.

80

81   **Primary human bronchial epithelial cell (HBEC) culture**

82   HBECs isolated from lungs not used for transplantation were cultured at air-liquid interface (ALI)

83   as previously described (16, 17). We harvested cells 23 days after establishment of ALI. Some

84   cultures were stimulated with IL-13 10 ng/ml for the final seven days of culture to induce goblet

85   cell production as indicated (18). The UCSF Committee on Human Research approved the use

86   of HBECs for these studies.

87

88   **Flow cytometry analysis**

89   We trypsinized HBECs to generate single cell suspensions and fixed cells in 0.5% (v/v)

90   paraformaldehyde; if not stained immediately, cells were frozen at -80 °C. Cells were blocked,

91   stained with the analytical panel (Table E1), and analyzed by flow cytometry.

92

93   **Flow cytometry cell sorting**

94   Prior to trypsinization, cells were incubated in culture media containing SiR-Tubulin

95   (Spirochrome/Cytoskeleton Inc., Denver, CO). Single cell suspensions were generated as

96   above, and singlets stained with fixable viability dye eFluor450 (ThermoFisher Scientific,

97   Fremont, CA, USA) to discriminate live cells. Cells were subsequently stained with a sorting

98   panel comprising cell surface markers only (Table E1) and sorted by flow cytometry.

99

100   **Gene expression analysis**

101   We isolated total RNA from sorted cells, performed reverse transcription, and analyzed the

102   cDNA by quantitative real-time PCR (qRT-PCR) to quantify specific mRNAs and microRNAs

103   (miRNAs). Table E2 lists qRT-PCR primer sequences.

104

105   **Results**

106   **Identification of airway epithelial subset markers**

107   To identify a panel of candidate cell-subset specific markers, we combined markers previously

108   used for flow cytometry (TUBA, ITGA6, NGFR, and ITGA6) with transcripts identified in several

109   recent human scRNA-seq datasets (cadherin-related family member 3 (CDHR3) and CEA cell

110   adhesion molecule (CEACAM) 5) (7, 9–11). We also analyzed HBECs differentiated at air-liquid

111   interface (16, 17) using the Drop-seq scRNA-seq platform (19); IL-13-stimulated cultures were

112   included as IL-13 induces goblet cell production (18) (Figure E1B). We examined our dataset for

113   cell-type–specific transcripts (Figure E1B), defined as genes more highly expressed in one cell

114   type than the others (FDR < 0.05) and identified two additional markers (CEACAM6 and

115   tetraspanin-8 (TSPAN8)). We combined all markers into a prospective flow panel (Table 1).

116   To test whether these putative cell subset markers were suitable for flow cytometry, we

117   stained unstimulated and IL-13–stimulated HBECs from 5 donors with antibodies against these

118   markers individually and performed flow cytometry. Each antibody stained a subset of HBECs

119   from both unstimulated and IL-13–stimulated cell cultures, except for the goblet cell markers

120   TSPAN8 and MUC5AC, which stained a subset of cells from IL-13–stimulated cultures, but few

121   if any cells from unstimulated cultures (Figure 1A). We observed significant increases in cells

122   staining for TSPAN8 (P = 0.022), and MUC5AC (P = 0.0016) following IL-13-stimulation;

123   however, we did not observe statistically significant effects of IL-13-stimulation on the proportion

124   of cells stained for the other markers (Figure 1B).

125

126   **Characterization of airway epithelial cells subsets using an analytical antibody panel**

127   To define the relationships between cell subsets defined by these eight individual

128   markers, we performed multicolor flow cytometry with an analytical panel comprising all eight

129   antibodies (Table E1) on unstimulated and IL-13–stimulated HBECs from three donors. This

130   produced a 10-dimensional dataset (one fluorescence intensity for each of the eight antibodies,

131   forward scatter (FSC), and side scatter (SSC)). We analyzed this dataset with t-Distributed

132   Stochastic Neighbor Embedding (tSNE; Figure 2A-J). The distribution of marker staining

133   indicated that cell type heterogeneity was the major driver of staining patterns in this data set,

134   although effects of IL-13-stimulation (Figure 2K) and inter-donor variation (Figure 2L) also

135   contributed to the staining patterns. We next examined each staining parameter in relation to

136   the tSNE plot. TUBA staining (Figure 2A) was confined to a distinct cluster of cells that were

137   predominantly CDHR3$^+$ (Figure 2B); cells bearing these two ciliated cell markers had little if any

138   basal or secretory cell marker staining. Another cluster comprised cells stained for the basal cell

139   markers NGFR (Figure 2C) and ITGA6 (Figure 2D), but with little if any secretory or ciliated cell

140   marker staining, except for a small subset that stained for CDHR3. Cells that stained for neither

141   ciliated nor basal cell markers generally stained with antibodies against one or both of the

142   secretory cell markers CEACAM5 (Figure 2E) and CEACAM6 (Figure 2F). CEACAM5 staining

143   was more pronounced in IL-13–stimulated cells. TSPAN8 and MUC5AC were detected only

144   after IL-13 stimulation. TSPAN8 staining was limited to a subset of CEACAM5$^+$ cells (Figure

145   2G); MUC5AC staining was confined to a subset of the TSPAN8$^+$ population (Figure 2H).

146   Ciliated cells (TUBA$^+$ and CDHR3$^+$) and some secretory cells tended to have higher forward

147   scatter (Figure 2I), an indicator of cell size, and basal cells (ITGA6$^+$ and frequently NGFR$^+$)

148   tended to have lower side scatter (Figure 2J).

149   To explore cellular heterogeneity, we examined the combination of the eight analytical

150   panel markers on individual cells. Figure 2M-Q and Figure E2 illustrate the use of a sequential

151   gating strategy to identify subpopulations of cells. Cells expressing the ciliated cell marker

152   TUBA were clearly distinct from those expressing the basal cell marker NGFR, and cells lacking

153   both TUBA and NGFR included subsets of cells expressing various combinations of the

154   secretory cell markers CEACAM6, TSPAN8, and MUC5AC that were markedly altered by IL-13

155   stimulation.

156   We considered all 2^8 (256) possible combinations of staining that could be seen using

157   the panel of 8 markers and focused our attention on all subsets containing at least 1% of total

158   cells (Figure 2R and Table E3). In unstimulated HBECs, 12 such subsets were observed. After

159   IL-13 stimulation, we identified 17 subsets, 11 of which were present in unstimulated culture

160   conditions. Subsets expressing basal cell markers (NGFR$^+$ITGA6$^+$, CDHR3$^+$NGFR$^+$ITGA6$^+$, and

161   ITGA6$^+$ only) were identified in both culture conditions and their proportions were not

162   significantly changed by IL-13. TUBA$^+$CDHR3$^+$ cells and TUBA$^+$ only cells were also present in

163   both unstimulated and IL-13-stimulated cultures, although the TUBA$^+$ only subset was

164   significantly reduced following IL-13-stimulation. Four TUBA$^+$CDHR3$^+$ cell subsets that co-

165   stained with combinations of the secretory cell markers CEACAM6, CEACAM5, and MUC5AC

166   were also observed; three of these subsets were significantly increased by IL-13. Cells

167   expressing both ciliated and secretory cell markers have been also identified in scRNA-seq

168   experiments, with pseudotime analyses suggesting that these cells may represent a transition

169   from secretory to ciliated cells (11). Of cells bearing secretory cell markers,

170   CEACAM6$^+$CEACAM5$^+$ cells were present in similar proportions in unstimulated and IL-13-

171   stimulated conditions, as were CEACAM5$^+$ only cells. CEACAM6$^+$ only cells were unique to

172   unstimulated cultures. IL-13 stimulation led to the emergence of cells expressing both

173   CEACAM5 and TSPAN8. These cells could be further subdivided into five subsets based on

174   expression of other markers. Three of the five CEACAM5⁺TSPAN8⁺ subsets also stained with

175   MUC5AC, as would be expected for goblet cells. Whether the CEACAM5⁺TSPAN8⁺MUC5AC⁻

176   populations represent goblet cell precursors, goblet cells that have secreted MUC5AC, or novel

177   IL-13–induced secretory cell subsets requires further investigation. Our findings are consistent

178   with bronchial tissue staining that demonstrated colocalization of CEACAM5 and MUC5AC in

179   never and current smokers (10). We also identified a subset that stained with none of the

180   markers (Null) and was present under both culture conditions. Collectively, these data suggest

181   IL-13 alters epithelial cell diversity, shifting populations towards cell subsets exhibiting secretory

182   and goblet cell markers.

183

184   **A modified flow cytometry panel is suitable for live cell sorting**

185   Flow cytometry is also useful for live cell sorting. Our analytical panel precludes this

186   since it requires fixation and permeabilization for staining with antibodies against the

187   intracellular antigens MUC5AC and TUBA. We therefore designed a sorting panel that omitted

188   the MUC5AC antibody and replaced the TUBA antibody with SiR-tubulin, a membrane-

189   permeable live cell dye that stains microtubules (20), which have a major structural role in cilia

190   (21). To ensure that we only sorted live cells, we also included a viability dye. The sorting panel

191   is detailed in Table E1.

192   To evaluate this panel, we performed flow cytometric cell sorting on unfixed HBECs from

193   3 donors (Figure 3A-E). After excluding dead cells that failed to exclude the viability dye, we

194   gated on SiR-tubulin and NGFR and identified the SiR-tubulin⁺NGFR⁻ singlets. Sorted SiR-

195   tubulin⁺NGFR⁻ cells were subsequently stained for TUBA and examined by microscopy; 58/60

196   cells examined possessed cilia and stained with TUBA, confirming that these were ciliated cells

197   (Figure 3F and G). We gated the remaining singlets on CEACAM6 and NGFR staining to

198   discriminate between secretory and basal cell subpopulations.

199   We sorted these three cell subsets from HBECs, isolated total RNA, and performed

200   qRT-PCR for cell type-specific markers (Figure 3H). As expected, the ciliated cell transcripts

201   forkhead box J1 (*FOXJ1*), tubulin alpha 1A class 1 (*TUBA1A*), and *CDHR3* were enriched in the

202   SiR-tubulin$^+$ ciliated cell subset. The basal cell transcripts cytokeratin 5 (*KRT5*) and *NGFR* were

203   enriched in the NGFR$^+$ basal cell subset; this subset also expressed *ITGA6*. The secretory cell

204   transcripts, secretoglobulin family 1A member 1 (*SCGB1A*, also known as club-cell specific

205   protein, *CCSP*) and mucin-5B (*MUC5B*), along with *CEACAM6*, were enriched in the

206   CEACAM6$^+$ secretory cell subset, as expected. The goblet cell transcripts SAM pointed domain

207   containing ETS transcription factor (*SPDEF*), *MUC5AC*, and *TSPAN8* were upregulated in

208   CEACAM6$^+$TSPAN8$^+$ cells from IL-13– stimulated HBEC cultures. Collectively, this analysis

209   demonstrated that the combination of cell surface marker and SiR-tubulin staining was sufficient

210   for discriminating the major airway epithelial cell populations.

211   Analyzing sorted cells may improve the ability to detect low abundance transcripts that

212   are difficult to quantify using available scRNA-seq approaches. We identified several transcripts

213   detected in a bulk RNA-seq dataset (22) but absent from our scRNA-seq dataset, and

214   performed qRT-PCR to determine their cell-subset–specific expression. For example, the

215   transcription factor *SPDEF* is critical for IL-13–induced goblet cell differentiation of HBECs (15)

216   but was not detected in our scRNA-seq dataset. Using our sorting panel, we found that *SPDEF*

217   was selectively expressed in CEACAM6$^+$ secretory cells, particularly CEACAM6$^+$TSPAN8$^+$ cells

218   (Figure 3D). The alarmin thymic stromal lymphopoietin (*TSLP*) was almost exclusively

219   expressed in the NGFR$^+$ basal cell subset. The ciliated cell transcription factor MYB proto-

220   oncogene, transcription factor (*MYB*) (23) was expressed primarily in SiR-tubulin$^+$ ciliated cells

221   and was downregulated by IL-13. Expression of the secreted protein, proline-rich protein BstNI

222   subfamily 1 (*PRB1*), which we identified as an IL-13-induced gene by bulk RNA-seq but did not

223   detect using Drop-seq, was enriched in the CEACAM6$^+$TSPAN8$^+$ secretory cell subset.

224   Analyzing sorted cells also allows for analysis of small RNAs, such as miRNAs, that are

225   not assessed using Drop-seq and related scRNA-seq approaches. miR-34/449 family miRNAs

226   are required for motile ciliogenesis (24). We quantified miR-34c-5p and miR-449a and

227   confirmed enrichment in SiR-tubulin$^+$ ciliated cells. We found that miR-375, which is involved in

228   goblet cell differentiation in the colon (25), was IL-13–inducible, restricted to secretory cells, and

229   enriched in the TSPAN8$^+$ secretory cell subset. These data demonstrate that the sorting

230   strategy we developed is useful for isolating and characterizing subpopulations of epithelial cells

231   with distinct transcriptional and miRNA profiles.

232

233   **Discussion**

234   Our study outlines an analytical flow panel and gating strategy for the characterization and

235   enumeration of subsets of airway epithelial cells from HBECs. We also demonstrate a scheme

236   for isolating common airway epithelial subsets from HBECs using a sorting flow panel. Both

237   panels identified the major airway epithelial subsets – ciliated cells, basal cells, and secretory

238   cells – as well as molecularly distinct subsets of each.

239   We identified several molecularly distinct, IL-13–regulated secretory cell subsets. IL-13-

240   driven changes included the disappearance of CEACAM6$^+$ only cells, and the emergence of

241   TSPAN8$^+$ and MUC5AC$^+$ subsets, supporting evidence of IL-13–induced alterations in secretory

242   cell phenotype. We confirm that transcriptional heterogeneity in secretory cells is accompanied

243   by related changes at the protein level. Whether these subsets are functionally disparate or

244   represent novel subsets with overlapping function, and what epigenetic processes underlie the

245   shift in secretory cell heterogeneity require further investigation. Understanding secretory cell

246   diversity in the context of IL-13 stimulation will be crucial in understanding asthma pathology.

247   Our data underline the increasing recognition of epithelial cell heterogeneity, suggesting

248   that airway epithelial subsets may be more precisely described by sets of molecular markers

249   rather than using traditional approaches for defining ciliated, basal and secretory cells based on

250   morphology and/or use of more limited sets of markers (26). Traditionally, nomenclature is

251   based principally on histologic criteria (5, 6) that fail to capture the heterogeneity evident from

252   scRNA-seq (7–11) or antibody panels. Our protocol provides a working method for classifying

253   airway epithelial subsets, and we expect that additional reagents can be added to this panel to

254   further subdivide major subsets and identify other smaller populations, such as ionocytes.

255   Furthermore, use of standard sets of molecular markers such as those developed here will

256   promote clearer communication and allow for more meaningful comparisons across studies.

257   We coupled flow cytometric cell sorting with gene expression analysis and identified

258   mRNA transcripts not detected in our scRNA-seq experiment plus several miRNAs. Although

259   scRNA-seq is revealing airway epithelial cell transcriptomes in unprecedented resolution,

260   current technologies have limited sensitivity and do not reliably detect low-abundance

261   transcripts (e.g. transcription factors) that may have significant impact on cell specification and

262   in disease. Furthermore, available scRNA-seq techniques are generally not suited for analyzing

263   mRNA variants or small RNAs, such as miRNAs. Therefore, our sorting panel may contribute to

264   deeper cataloging of airway epithelial subset transcriptomes. Additionally, our panels could be

265   coupled with downstream epigenetic and proteomic analyses to further understand the

266   specification and/or function of airway epithelial subsets in human health and disease.

267   There is also potential to build on the protocols we have developed. For example,

268   although flow cytometric analysis of clinical samples was not performed, published scRNA-seq

269   datasets suggest that the panels we developed could be useful for analyzing disaggregated

270   cells from human airways (7, 9–11). Furthermore, although our study used a 10-parameter, 8-

271   fluorochrome approach, application of an increased panel is viable. Future refinement and the

272   addition of other markers for rarer epithelial subtypes (e.g. cystic fibrosis transmembrane

273   conductance regulator (CFTR)-expressing ionocytes and doublecortin like kinase 1 (DCLK1)-

274   expressing tuft cells (7–10)) may permit characterization of the null or minor (<1%) populations

275   reported here. Additionally, combining the epithelial panel with existing panels for immune cells

276   and other non-epithelial cells will permit a more comprehensive examination of lung

277   development, airway inflammatory and immune responses, and a variety of disease states.

278   Mass cytometry (27) or use of oligonucleotide-barcoded antibodies together with single cell

279   sequencing (28) also promise to allow for more extensive panels of markers that could further

280   expand our approach to increase our understanding of the function of specific subsets and their

281   heterogeneity.

282   In summary, we have leveraged scRNA-seq datasets to develop flow cytometry panels

283   for characterizing subpopulations of airway epithelial cells. These panels identified major airway

284   epithelial cell subsets, revealed molecular heterogeneity within these populations, and permitted

285   analysis of low abundance transcripts and miRNAs. We envisage that these panels and their

286   future refinements will be powerful tools for interrogating airway epithelial biology.

287

288   **Acknowledgements**

References

1. Maecker HT, McCoy JP, Nussenblatt R. Standardizing immunophenotyping for the Human Immunology Project. *Nature Reviews Immunology* 2012;12:191–200.

2. Tighe RM, Redente EF, Yu Y-R, Herold S, Sperling AI, Curtis JL, Duggan R, Swaminathan S, Nakano H, Zacharias WJ, Janssen WJ, Freeman CM, Brinkman RR, Singer BD, Jakubzick CV, Misharin AV. Improving the Quality and Reproducibility of Flow Cytometry in the Lung. An Official American Thoracic Society Workshop Report. *Am J Respir Cell Mol Biol* 2019;61:150–161.

3. Bonser LR, Erle DJ. The airway epithelium in asthma. *Adv Immunol* 2019;142:1–34.

4. Bonser LR, Erle DJ. Airway Mucus and Asthma: The Role of MUC5AC and MUC5B. *J Clin Med* 2017;6:.

5. Rhodin J. LXVII Ultrastructure of the Tracheal Ciliated Mucosa in Rat and Man. *Annals of Otology, Rhinology & Laryngology* 1959;68:964–974.

6. Widdicombe JH. Early Studies on the Surface Epithelium of Mammalian Airways. *American Journal of Physiology-Lung Cellular and Molecular Physiology* 2019;doi:10.1152/ajplung.00240.2019.

7. Plasschaert LW, Žilionis R, Choo-Wing R, Savova V, Knehr J, Roma G, Klein AM, Jaffe AB. A single-cell atlas of the airway epithelium reveals the CFTR-rich pulmonary ionocyte. *Nature* 2018;560:377.

8. Montoro DT, Haber AL, Biton M, Vinarsky V, Lin B, Birket SE, Yuan F, Chen S, Leung HM, Villoria J, Rogel N, Burgin G, Tsankov AM, Waghray A, Slyper M, Waldman J, Nguyen L, Dionne D, Rozenblatt-Rosen O, Tata PR, Mou H, Shivaraju M, Bihler H, Mense M, Tearney GJ, Rowe SM, Engelhardt JF, Regev A, Rajagopal J. A revised airway epithelial hierarchy includes CFTR-expressing ionocytes. *Nature* 2018;560:319.

316   9. Ordovas-Montanes J, Dwyer DF, Nyquist SK, Buchheit KM, Vukovic M, Deb C, Wadsworth

317   MH, Hughes TK, Kazer SW, Yoshimoto E, Cahill KN, Bhattacharyya N, Katz HR, Berger B,

318   Laidlaw TM, Boyce JA, Barrett NA, Shalek AK. Allergic inflammatory memory in human

319   respiratory epithelial progenitor cells. *Nature* 2018;560:649.

320   10. Duclos GE, Teixeira VH, Autissier P, Gesthalter YB, Reinders-Luinge MA, Terrano R,

321   Dumas YM, Liu G, Mazzilli SA, Brandsma C-A, Berge M van den, Janes SM, Timens W,

322   Lenburg ME, Spira A, Campbell JD, Beane J. Characterizing smoking-induced

323   transcriptional heterogeneity in the human bronchial epithelium at single-cell resolution.

324   *Science Advances* 2019;5:eaaw3413.

325   11. García SR, Deprez M, Lebrigand K, Cavard A, Paquet A, Arguel M-J, Magnone V, Truchi M,

326   Caballero I, Leroy S, Marquette C-H, Marcet B, Barbry P, Zaragosi L-E. Novel dynamics of

327   human mucociliary differentiation revealed by single-cell RNA sequencing of nasal epithelial

328   cultures. *Development* 2019;146:.

329   12. Maestre-Batlle D, Pena OM, Hirota JA, Gunawan E, Rider CF, Sutherland D, Alexis NE,

330   Carlsten C. Novel flow cytometry approach to identify bronchial epithelial cells from healthy

331   human airways. *Sci Rep* 2017;7:1–9.

332   13. Griggs TF, Bochkov YA, Basnet S, Pasic TR, Brockman-Schneider RA, Palmenberg AC,

333   Gern JE. Rhinovirus C targets ciliated airway epithelial cells. *Respir Res* 2017;18:84.

334   14. Rock JR, Onaitis MW, Rawlins EL, Lu Y, Clark CP, Xue Y, Randell SH, Hogan BLM. Basal

335   cells as stem cells of the mouse trachea and human airway epithelium. *PNAS*

336   2009;106:12771–12775.

337   15. Koh KD, Siddiqui S, Cheng D, Bonser LR, Sun DI, Zlock LT, Finkbeiner WE, Woodruff PG,

338   Erle DJ. Efficient RNP-Directed Human Gene Targeting Reveals SPDEF is Required for IL-

339   13-Induced Mucostasis. *Am J Respir Cell Mol Biol* 2019;doi:10.1165/rcmb.2019-0266OC.

340   16. Fulcher ML, Gabriel S, Burns KA, Yankaskas JR, Randell SH. Well-Differentiated Human

341   Airway Epithelial Cell Cultures. In: Picot J, editor. *Human Cell Culture Protocols* Totowa, NJ:

342   Humana Press; 2005. p. 183–206.doi:10.1385/1-59259-861-7:183.

343   17. Whitcutt MJ, Adler KB, Wu R. A biphasic chamber system for maintaining polarity of

344   differentiation of cultured respiratory tract epithelial cells. *In Vitro Cell Dev Biol* 1988;24:420–

345   428.

346   18. Bonser LR, Zlock L, Finkbeiner W, Erle DJ. Epithelial tethering of MUC5AC-rich mucus

347   impairs mucociliary transport in asthma. *J Clin Invest* 2016;126:2367–2371.

348   19. Macosko EZ, Basu A, Satija R, Nemesh J, Shekhar K, Goldman M, Tirosh I, Bialas AR,

349   Kamitaki N, Martersteck EM, Trombetta JJ, Weitz DA, Sanes JR, Shalek AK, Regev A,

350   McCarroll SA. Highly Parallel Genome-wide Expression Profiling of Individual Cells Using

351   Nanoliter Droplets. *Cell* 2015;161:1202–1214.

352   20. Lukinavičius G, Reymond L, D'Este E, Masharina A, Göttfert F, Ta H, Güther A, Fournier M,

353   Rizzo S, Waldmann H, Blaukopf C, Sommer C, Gerlich DW, Arndt H-D, Hell SW, Johnsson

354   K. Fluorogenic probes for live-cell imaging of the cytoskeleton. *Nature Methods*

355   2014;11:731–733.

356   21. Oltean A, Schaffer AJ, Bayly PV, Brody SL. Quantifying Ciliary Dynamics during Assembly

357   Reveals Stepwise Waveform Maturation in Airway Cells. *Am J Respir Cell Mol Biol*

358   2018;59:511–522.

359   22. Christenson SA, van den Berge M, Faiz A, Inkamp K, Bhakta N, Bonser LR, Zlock LT,

360   Barjaktarevic IZ, Barr RG, Bleecker ER, Boucher RC, Bowler RP, Comellas AP, Curtis JL,

361   Han MK, Hansel NN, Hiemstra PS, Kaner RJ, Krishnanm JA, Martinez FJ, O'Neal WK,

362   Paine R, Timens W, Wells JM, Spira A, Erle DJ, Woodruff PG. An airway epithelial IL-17A

363   response signature identifies a steroid-unresponsive COPD patient subgroup. *J Clin Invest*

364   2019;129:169–181.

365   23. Pan J, Adair-Kirk TL, Patel AC, Huang T, Yozamp NS, Xu J, Reddy EP, Byers DE, Pierce

366   RA, Holtzman MJ, Brody SL. Myb permits multilineage airway epithelial cell differentiation.

367   *Stem Cells* 2014;32:3245–3256.

368   24. Song R, Walentek P, Sponer N, Klimke A, Lee JS, Dixon G, Harland R, Wan Y, Lishko P,

369   Lize M, Kessel M, He L. miR-34/449 miRNAs are required for motile ciliogenesis by

370   repressing cp110. *Nature* 2014;510:115–120.

371   25. Biton M, Levin A, Slyper M, Alkalay I, Horwitz E, Mor H, Kredo-Russo S, Avnit-Sagi T,

372   Cojocaru G, Zreik F, Bentwich Z, Poy MN, Artis D, Walker MD, Hornstein E, Pikarsky E,

373   Ben-Neriah Y. Epithelial microRNAs regulate gut mucosal immunity via epithelium–T cell

374   crosstalk. *Nature Immunology* 2011;12:239–246.

375   26. Bonser LR, Erle DJ. Putting Mucins on the Map. *American Journal of Respiratory and

376   Critical Care Medicine* 2018;doi:10.1164/rccm.201809-1818ED.

377   27. Bandura DR, Baranov VI, Ornatsky OI, Antonov A, Kinach R, Lou X, Pavlov S, Vorobiev S,

378   Dick JE, Tanner SD. Mass cytometry: technique for real time single cell multitarget

379   immunoassay based on inductively coupled plasma time-of-flight mass spectrometry. *Anal

380   Chem* 2009;81:6813–6822.

381   28. Akkaya B, Miozzo P, Holstein AH, Shevach EM, Pierce SK, Akkaya M. A Simple, Versatile

382   Antibody-Based Barcoding Method for Flow Cytometry. *The Journal of Immunology*

383   2016;197:2027–2038.

384   29. Piperno G, Fuller MT. Monoclonal antibodies specific for an acetylated form of alpha-tubulin

385   recognize the antigen in cilia and flagella from a variety of organisms. *J Cell Biol*

386   1985;101:2085–2094.

387   30. Basnet S, Bochkov YA, Brockman-Schneider RA, Kuipers I, Aesif SW, Jackson DJ,

388   Lemanske RF, Ober C, Palmenberg AC, Gern JE. CDHR3 Asthma-Risk Genotype Affects

389   Susceptibility of Airway Epithelium to Rhinovirus C Infections. *Am J Respir Cell Mol Biol*

390   2019;61:450–458.

391   31. Bønnelykke K, Sleiman P, Nielsen K, Kreiner-Møller E, Mercader JM, Belgrave D, den

392   Dekker HT, Husby A, Sevelsted A, Faura-Tellez G, Mortensen LJ, Paternoster L, Flaaten R,

393   Mølgaard A, Smart DE, Thomsen PF, Rasmussen MA, Bonàs-Guarch S, Holst C, Nohr EA,

394   Yadav R, March ME, Blicher T, Lackie PM, Jaddoe VWV, Simpson A, Holloway JW, Duijts

395   L, Custovic A, *et al.* A genome-wide association study identifies CDHR3 as a susceptibility

396   locus for early childhood asthma with severe exacerbations. *Nat Genet* 2014;46:51–55.

397   32. Beane J, Sebastiani P, Liu G, Brody JS, Lenburg ME, Spira A. Reversible and permanent

398   effects of tobacco smoke exposure on airway epithelial gene expression. *Genome Biol*

399   2007;8:R201.

400   33. Ooi AT, Gower AC, Zhang KX, Vick JL, Hong L, Nagao B, Wallace WD, Elashoff DA,

401   Walser TC, Dubinett SM, Pellegrini M, Lenburg ME, Spira A, Gomperts BN. Molecular

402   Profiling of Premalignant Lesions in Lung Squamous Cell Carcinomas Identifies

403   Mechanisms Involved in Stepwise Carcinogenesis. *Cancer Prev Res* 2014;7:487–495.

404   34. Shikotra A, Choy DF, Siddiqui S, Arthur G, Nagarkar DR, Jia G, Wright AKA, Ohri CM,

405   Doran E, Butler CA, Hargadon B, Abbas AR, Jackman J, Wu LC, Heaney LG, Arron JR,

406   Bradding P. A CEACAM6-High Airway Neutrophil Phenotype and CEACAM6-High Epithelial

407   Cells Are Features of Severe Asthma. *J Immunol* 2017;198:3307–3317.

408

409 **Table 1. Panel of cell-subset–specific markers**

Name	Antigen	Cell subset	Description	References
Acetylated alpha-tubulin	TUBA	Ciliated	Recognizes axonemal alpha-tubulin acetylated on the epsilon-amino group of lysine(s), a hallmark of stable microtubules, which are enriched in motile cilia	(7, 9, 10, 21, 29)
Cadherin-related family member 3	CDHR3	Ciliated	Calcium-dependent cell adhesion protein associated with ciliogenesis and asthma; receptor for Rhinovirus C	(9, 10, 13, 30, 3
integrin subunit alpha 6	CD49f/ ITGA6	Basal	Integral membrane protein of the integrin alpha chain family; function uncharacterized in the airway	(10, 14)
Nerve growth factor receptor	CD271/ NGFR	Basal	Cell surface receptor localized to basal cells of unknown function in the airway	(7, 14)
CEA cell adhesion molecule 5	CD66c/ CEACAM5	Secretory	Cell surface glycoprotein upregulated after smoking cessation and linked to lung squamous cell carcinoma	(9, 10, 32, 33)
CEA cell adhesion molecule 6	CD66e/ CEACAM6	Secretory	Cell surface glycoprotein associated with severe asthma and upregulated after smoking cessation	(7, 9, 10, 32, 34)
Tetraspanin 8	TSPAN8	Goblet	Cell surface glycoprotein of unknown function in the airway	(9, 10)
Mucin 5AC	MUC5AC	Goblet	Secreted, gel-forming glycoprotein associated with mucus dysfunction in chronic lung disease	(4, 9, 10)

410

411 **Figure Legends**

412 **Figure 1: Identification of cell-specific markers for flow cytometry.** (*A*) Human bronchial

413 epithelial cells (HBECs) grown in the absence (cyan histogram) or presence of interleukin-13

414 (IL-13; magenta histogram) were stained using antibodies against cell subset specific markers.

415 Positive staining was determined by comparing the same sample stained with an appropriate

416 isotype control (grey histogram). (*B*) Comparison of positive staining for cell-subset–specific

417 markers from unstimulated and IL-13–stimulated HBECs (n=5; each donor is represented by a

418 different color). Significance was evaluated using a *t*-test: ns, nonsignificant; *, $P < 0.05$; and **,

419 $P < 0.01$.

420

421 **Figure 2: Characterization of airway epithelial cells subsets and IL-13 stimulation using**

422 **an analytical flow cytometry panel.** HBECs (n=3) were cultured with or without IL-13 and then

423 processed for multicolor flow cytometry. (*A-L*) Results from 3,000 cells from each donor were

424 combined and analyzed by t-Distributed Stochastic Neighbor Embedding (tSNE). tSNE plots are

425 colored to show cells that stained for the ciliated cell markers (red) TUBA (*A*) and CDHR3 (*B*),

426 the basal cell markers (blue) NGFR (*C*) and ITGA6 (*D*), and the secretory cell markers (green)

427 CEACAM6 (*E*), CEACAM5 (*F*), TSPAN8 (*G*), and MUC5AC (*H*). Forward scatter FSC (*J*) and

428 side scatter SSC (*K*) are represented as a continuum from low (blue) to high (red). Cells came

429 from unstimulated (-) or IL-13-stimulated cultures (*K*) from three donors (*L*). (*M-Q*) Gating

430 strategy to identify airway epithelial subsets from unstimulated (IL-13-) and IL-13–stimulated (IL-

431 13+) HBECs. Doublets (*M*) and debris (*N*) were removed, and resulting singlets were gated on

432 NGFR and TUBA (*O*). Subsequently, TUBA⁻NGFR⁻ singlets were gated on ITGA6 and

433 CEACAM6 (*P*). ITGA6⁻CEACAM6⁺ cells were then gated on MUC5AC and TSPAN8 (*Q*). (*R*)

434 Comparison of cell subsets (>1%) from unstimulated (IL-13-; cyan) and IL-13–stimulated (IL-

435 13+; magenta) HBECs (n=3; each donor is represented by a different point). Ciliated cell

436 markers are colored blue, basal cell markers red, and secretory cell markers green. "Null"

437 indicates cells that did not stain with any of the eight markers and "Other" indicates totals for all

438 subsets representing <1% of total cells. Significance was evaluated using Student's *t*-test: ns,

439 not significant; *, $P < 0.05$; **, $P < 0.01$.

440

441 **Figure 3: Flow cytometric sorting of HBEC subsets.** Prior to processing for flow cytometry,

442 HBECs cultured in the absence or presence of IL-13 were stained with SiR-tubulin. SiR-tubulin–

443 stained cells were trypsinized, stained with a cell viability dye, and sorted by FACS. (*A-E*)

444 Gating strategy for flow cytometric cell sorting of unstimulated (IL-13-) and IL-13–stimulated (IL-

445 13+) HBECs. After selection of singlets (*A*) and live cells (*B*), cells were gated on SiR-tubulin

446 and NGFR staining (*C*). SiR-tubulin⁻ cells were gated on NGFR and CEACAM6 (*D*). NGFR⁻

447 CEACAM6⁺ cells were gated on MUC5AC and TSPAN8 (*E*). (*F*, *G*) To validate SiR-tubulin

448 staining, SiR-tubulin⁺ cells were fixed in paraformaldehyde, immobilized to slides by cytospin,

449 stained with TUBA (cyan), and counterstained with DAPI (blue). Images show cells from

450 unstimulated (IL-13-, *F*) and IL-13–stimulated (IL-13+, *G*) cultures with TUBA-stained cilia

451 (found in 58/60 cells examined). Scale bar = 10 μM. (*H*) Quantitative real-time PCR analysis of

452 sorted cell subpopulations. Mean expression values calculated from triplicate experiments with

453 different donors were normalized to the maximum expression of the gene in any cell type (0-1:
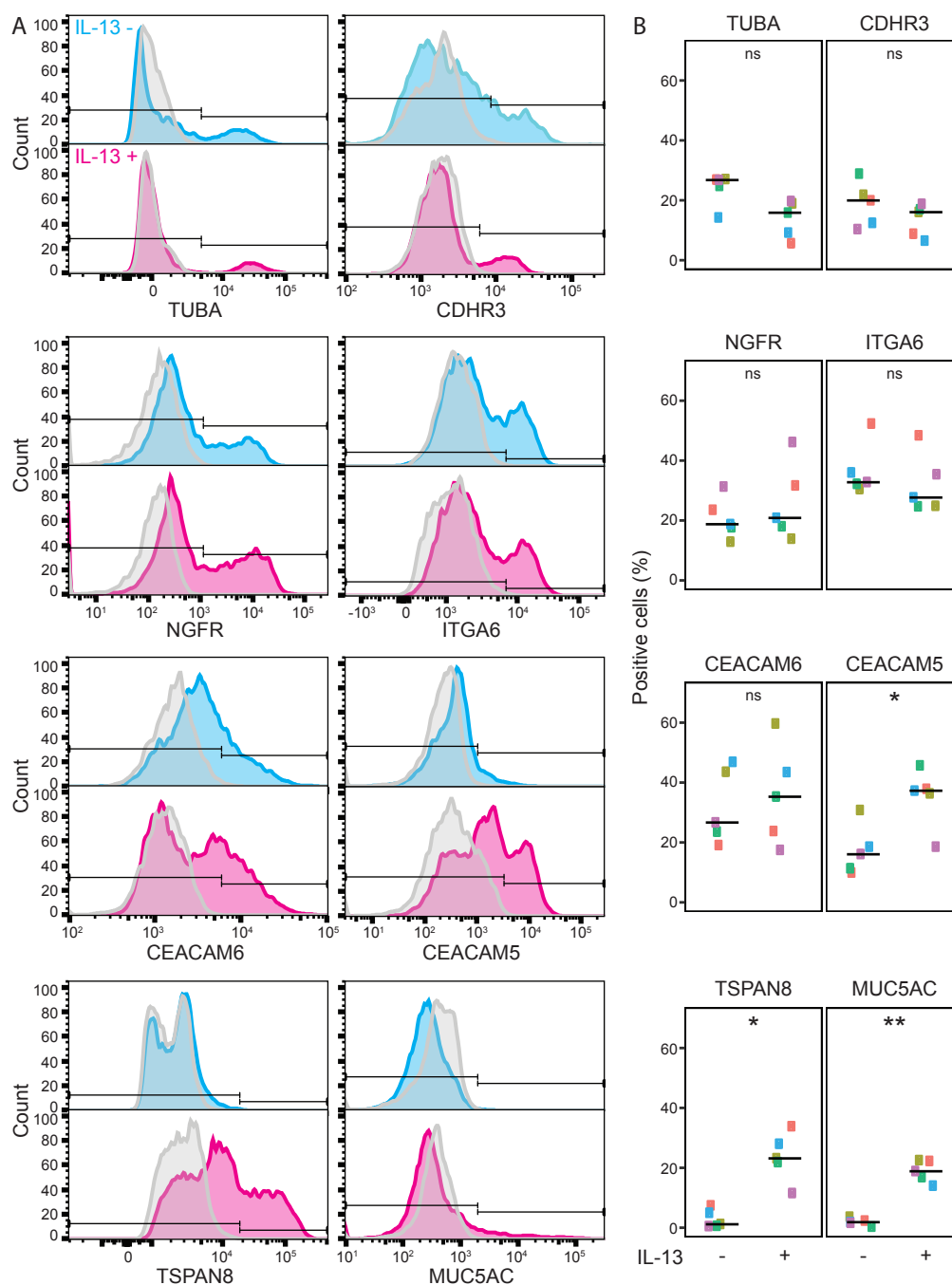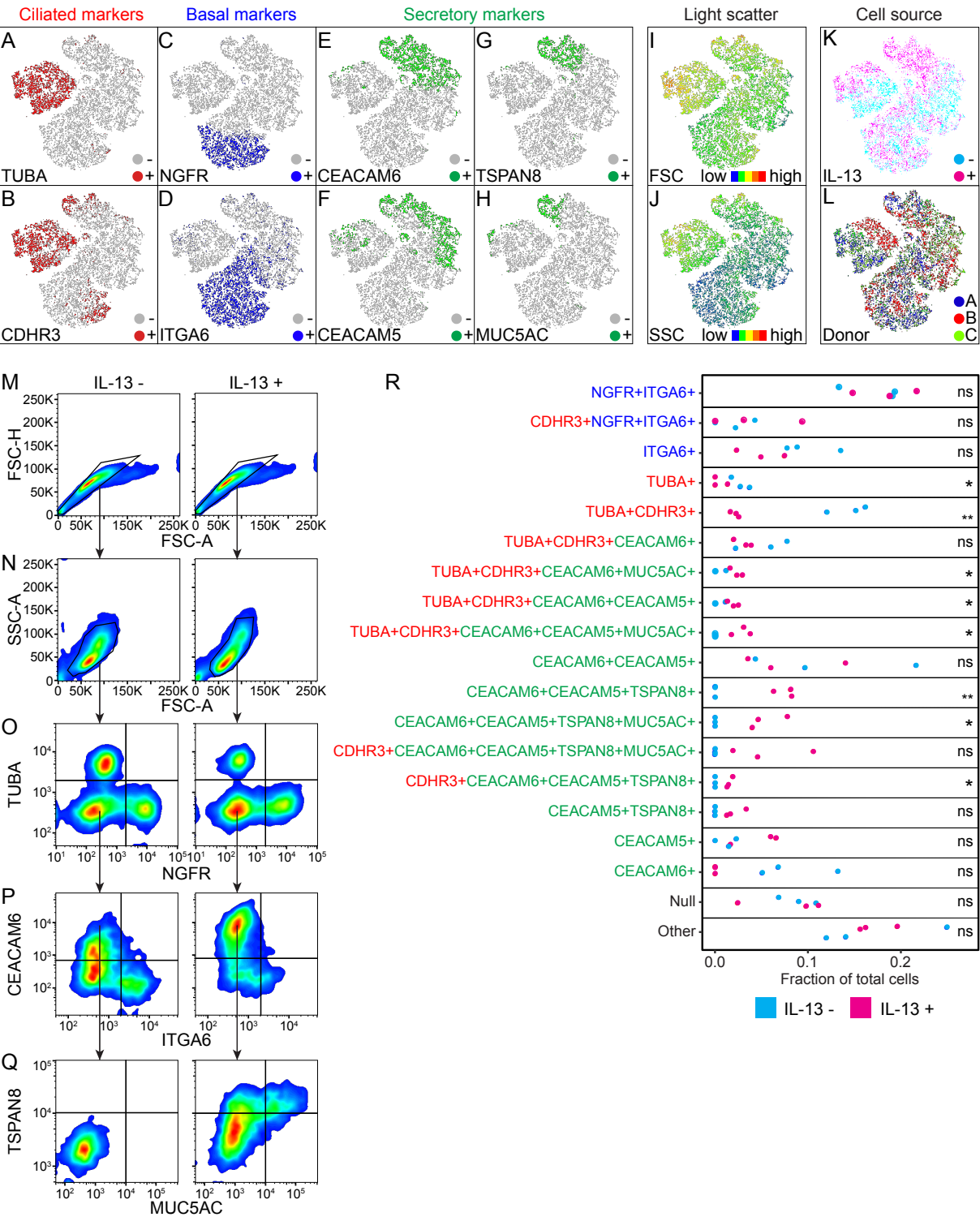
454 white-red).

Figure 1

Figure 2

Figure 3